

# A one-dimensional assembly of a square-planar copper(II) complex with alternating short and long Cu···Cu distances. Metal ion spin-exchange *via* $\pi$ - $\pi$ interactions

Sunirban Das, G. P. Muthukumaragopal, Satyanarayan Pal and Samudranil Pal\*

School of Chemistry, University of Hyderabad, Hyderabad 500 046, India

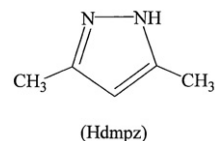
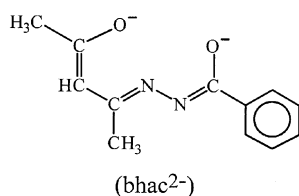
Received (in Montpellier, France) 13th December 2002, Accepted 5th March 2003

First published as an Advance Article on the web 13th June 2003

A mixed-ligand copper(II) complex, [Cu(bhac)(Hdmpz)], with a tridentate Schiff base, acetylacetone benzoylhydrazone (H<sub>2</sub>bhac) and a monodentate heterocycle, 3,5-dimethylpyrazole (Hdmpz), has been synthesized and characterized by analytical, infrared and electronic absorption spectroscopy, and cyclic voltammetry. The molecular structure of the complex has been determined by X-ray crystallography. The metal ion is coordinated to the enolate-O, the imine-N and the deprotonated amide-O centres of the deprotonated Schiff base (bhac<sup>2-</sup>) and to the sp<sup>2</sup> N atom of Hdmpz. The coordination geometry around the metal centre is square-planar. There is no displacement of the metal centre from the N<sub>2</sub>O<sub>2</sub> square plane. The whole molecule is essentially planar, barring a small variation in the orientation of the Hdmpz plane with respect to the {Cu(bhac)} plane. In the solid state, two types of  $\pi$ - $\pi$  interactions on two sides of [Cu(bhac)(Hdmpz)] molecule lead to a one-dimensional arrangement of the complex with sequential short [3.5952(8) Å] and long [5.5960(12) Å] Cu···Cu distances. Solid state as well as frozen solution EPR spectral measurements reveal an antiferromagnetically coupled dicopper(II) system and indicate a magnetic exchange interaction mediated by  $\pi$ - $\pi$  interactions. Magnetic susceptibility data in the temperature range of 10–300 K are consistent with this observation. The magnitude of the coupling constant *J*, obtained by least-squares fitting of the data using the Bleaney–Bowers expression, is  $-6.0(1) \text{ cm}^{-1}$ .

## Introduction

The study of supramolecular species involving metal ions is an area of immense research activity in recent times.<sup>1</sup> Interest in such species is primarily due to their possible applications as molecule-based metals and magnets, optical and thermal switches and as probes for DNA structures.<sup>1,2</sup> Self-assembly of transition metal ion complexes into supramolecular entities is generally achieved by utilizing the metal ion's preference for different coordination geometries, designing suitable ligands and using weak intermolecular interactions such as hydrogen bonding and  $\pi$ - $\pi$  interactions.<sup>1–3</sup> Recently, we have reported a one-dimensional array of a square-pyramidal copper(II) complex assembled *via* sequential hydrogen bonding and  $\pi$ - $\pi$  interactions with successive long (6.455 Å) and short (4.023 Å) Cu···Cu distances.<sup>4</sup> However, cryomagnetic studies showed a Curie paramagnetic behaviour of this complex in the solid state. Herein, we report a novel one-dimensional assembly of a square-planar copper(II) complex, [Cu(bhac)(Hdmpz)], formed *via* only  $\pi$ - $\pi$  interactions with similar successive long and short Cu···Cu distances. The ligands used are the dianionic O,N,O-donor deprotonated acetylacetone benzoylhydrazone (H<sub>2</sub>bhac) and the monodentate neutral N-donor 3,5-dimethylpyrazole (Hdmpz). EPR and cryomagnetic studies reveal an antiferromagnetic metal ion spin-coupling.



## Experimental

### Materials

The Schiff base, H<sub>2</sub>bhac, was prepared as before.<sup>5</sup> All other chemicals and solvents used in this work were of analytical grade available commercially and were used without further purification.

### Physical measurements

Microanalytical (C, H, N) data were obtained with a Perkin–Elmer Model 240C elemental analyser. The infrared spectrum was recorded by using a KBr pellet on a Jasco-5300 FT-IR spectrophotometer. Solution electrical conductivity was measured with a Digisun DI-909 conductivity meter. A Shimadzu 3101-PC UV/vis/NIR spectrophotometer was used to record the electronic spectrum. A CH-Instruments model 620A electrochemical analyser was used for the cyclic voltammetric experiments with a chloroform solution of the complex containing tetrabutylammonium perchlorate (TBAP) as supporting electrolyte. The three-electrode measurement was carried out at 298 K under a dinitrogen atmosphere with a platinum working electrode, a platinum wire auxiliary electrode and a saturated calomel reference electrode (SCE). The X-ray powder diffraction pattern was collected on a Philips PW-3710 diffractometer using Cu K $\alpha$  radiation ( $\lambda = 1.54184 \text{ Å}$ ). The EPR

spectra were recorded on a Jeol JES-FA200 spectrometer. The variable temperature (10–300 K) magnetic susceptibility measurements were performed using the Faraday technique with a set-up comprising a George Associates Lewis coil force magnetometer, a CAHN microbalance and an Air Products cryostat.  $\text{Hg}[\text{Co}(\text{NCS})_4]$  was used as the standard. A diamagnetic correction ( $-155 \times 10^{-6} \text{ emu mol}^{-1}$  for  $[\text{Cu}(\text{bhac})(\text{Hdmpz})]$ ) calculated from Pascal's constants,<sup>6</sup> was used to obtain the molar paramagnetic susceptibilities.

### Synthesis of $[\text{Cu}(\text{bhac})(\text{Hdmpz})]$

A dry ethanol solution (15 mL) of  $\text{Cu}(\text{O}_2\text{CCH}_3)_2 \cdot \text{H}_2\text{O}$  (199 mg, 1 mmol) was added to another dry ethanol solution (20 mL) of  $\text{H}_2\text{bhac}$  (261 mg, 1.2 mmol) and 3,5-dimethyl pyrazole (Hdmpz) (96 mg, 1 mmol). The resulting green mixture was stirred at room temperature for 2 h. The mixture was then evaporated on a steam bath to  $\sim 1/4$  of the original volume and slowly cooled to room temperature. The brown needles deposited were collected by filtration and dried in air. Yield, 320 mg (86%). A single crystal suitable for X-ray structure determination was selected from this material. Anal. calcd. for  $\text{C}_{17}\text{H}_{20}\text{N}_4\text{O}_2\text{Cu}$ : C, 54.32; H, 5.36; N, 14.90; found: C, 54.10; H, 5.34; N, 14.73. Selected IR bands ( $\text{cm}^{-1}$ ): 3310(m), 1597(s), 1568(m), 1512(s), 1489(m), 1412(s), 1346(w), 1269(s), 1209(w), 1169(m), 1140(w), 1065(w), 1036(s), 949(m), 789(s), 766(m), 687(s), 602(m), 567(w), 474(w), 438(s), 407(w). UV/Vis [ $\text{CHCl}_3$ ;  $\lambda_{\text{max}}/\text{nm}$  ( $\epsilon/\text{dm}^3 \text{ mol}^{-1} \text{ cm}^{-1}$ ): 577 (107), 373 (17 700), 360sh (16 900), 245 (20 400).

### X-Ray crystallography

A crystal of dimension  $0.48 \times 0.28 \times 0.24 \text{ mm}^3$  was used for data collection on an Enraf–Nonius Mach-3 single crystal diffractometer using graphite monochromated  $\text{Mo K}\alpha$  radiation ( $\lambda = 0.71073 \text{ \AA}$ ) by the  $\omega$ -scan method at 298 K. Unit cell parameters were determined by the least-squares fit of 25 reflections having  $\theta$  values in the range  $9\text{--}11^\circ$ . Intensities of 3 check reflections were measured every 1.5 h during the data collection to monitor the crystal stability. No decay was observed in 28 h of exposure. The  $\psi$ -scans of 6 reflections with  $\theta$  in the range  $5\text{--}21^\circ$  and  $\chi$  within  $80\text{--}89^\circ$  were used for an empirical absorption correction.<sup>7</sup> The structure was solved by direct methods in the  $P\bar{1}$  space group and refined on  $F^2$  by full-matrix least-squares procedures. The asymmetric unit contains a molecule of  $[\text{Cu}(\text{bhac})(\text{Hdmpz})]$ . All non-hydrogen atoms were refined using anisotropic thermal parameters. Hydrogen atoms were placed geometrically by using a riding model and included in the structure factor calculation, but not refined. Calculations were done using the programmes in WinGX<sup>8</sup> for data reduction and absorption correction, and the SHELX-97 programmes<sup>9</sup> for structure solution and refinement. Ortep6a<sup>10</sup> and Platon98<sup>11</sup> packages were used for molecular graphics. Significant crystal data are listed in Table 1.

CCDC reference number 202929. See <http://www.rsc.org/suppdata/nj/b2/b212399c/> for crystallographic files in CIF or other electronic format.

## Results and discussion

### Synthesis and characterization

In ethanolic medium, the reaction of  $\text{Cu}(\text{O}_2\text{CCH}_3)_2 \cdot \text{H}_2\text{O}$ ,  $\text{H}_2\text{bhac}$  and Hdmpz in a 1:1:1 mole ratio affords the green complex in good yield. Elemental analysis data are satisfactory with the formula  $[\text{Cu}(\text{bhac})(\text{Hdmpz})]$ . The complex is electrically non-conducting in acetonitrile solution.

The infrared spectrum of the complex does not display the amide  $\text{C}=\text{O}$  ( $\sim 1675 \text{ cm}^{-1}$ ) stretch<sup>12</sup> expected for the free  $\text{H}_2\text{bhac}$ . Thus, in the complex the metal ion is in a +2

**Table 1** Crystallographic data for  $[\text{Cu}(\text{bhac})(\text{Hdmpz})]$

Chemical formula	$\text{C}_{17}\text{H}_{20}\text{N}_4\text{O}_2\text{Cu}$
Formula weight	375.91
Crystal system	Triclinic
Space group	$P\bar{1}$
$T/\text{K}$	298
$a/\text{\AA}$	7.2563(13)
$b/\text{\AA}$	10.6168(16)
$c/\text{\AA}$	12.0608(19)
$\alpha/\text{deg}$	103.213(12)
$\beta/\text{deg}$	103.625(14)
$\gamma/\text{deg}$	101.443(13)
$U/\text{\AA}^3$	847.3(2)
$Z$	2
$\mu/\text{mm}^{-1}$	1.306
Total reflections	2980
Indep. reflections	2980
$R_{\text{int}}$	0.00
$R_1^a$ [ $I \geq 2\sigma(I)$ ]	0.0305
$wR_2^b$ [ $I \geq 2\sigma(I)$ ]	0.0779
$R_1^a$ (all data)	0.0398
$wR_2^b$ (all data)	0.0827

$$^a R_1 = \sum \|F_o| - |F_c|\| / \sum |F_o|, \quad ^b wR_2 = \{ \sum [(F_o^2 - F_c^2)^2] / \sum [w(F_o^2)^2] \}^{1/2}.$$

oxidation state and coordinated to the enolate-O, the imine-N and the deprotonated amide-O atoms of the completely deprotonated Schiff base ( $\text{bhac}^{2-}$ ). A strong peak observed at  $1597 \text{ cm}^{-1}$  is possibly associated with the  $\text{C}=\text{N}-\text{N}=\text{C}$  moiety of  $\text{bhac}^{2-}$ .<sup>13</sup> The fourth coordination site is satisfied by the imine-N of Hdmpz. The X-ray structure (*vide infra*) confirms such coordination of  $\text{bhac}^{2-}$  and Hdmpz and the +2 oxidation state of the metal ion. The sharp peak observed at  $3310 \text{ cm}^{-1}$  is assigned to the N–H group of Hdmpz.

The electronic spectrum of the complex in chloroform solution displays a weak band at 577 nm. Absorptions in this region observed for square-planar or square-pyramidal copper(II) Schiff base complexes have been assigned to d-d transitions.<sup>14</sup> The intense absorptions displayed in the range of 374–245 nm are likely to be due to ligand-to-metal charge transfer and intraligand transitions.

In chloroform solution, the complex is redox active. A cyclic voltammogram of the complex displays an irreversible oxidation at 0.77 V (*vs.* SCE). On the cathodic side of SCE (up to  $-1.0 \text{ V}$ ) no redox response is observed. The current height of the oxidation response is comparable with known one-electron redox processes under identical conditions.<sup>15</sup> No such response is observed for either deprotonated  $\text{bhac}^{2-}$  or Hdmpz under the same conditions. The iron(III) complex of  $\text{bhac}^{2-}$  displays a metal-centred one-electron oxidation response at 0.4 V.<sup>5</sup> Thus, the oxidation observed for  $[\text{Cu}(\text{bhac})(\text{Hdmpz})]$  is assigned to a  $\text{Cu(II)} \rightarrow \text{Cu(III)}$  process. The irreversible nature suggests that the corresponding oxidized species is unstable on the cyclic voltammetry time scale.

### Description of molecular structure

The molecular structure of  $[\text{Cu}(\text{bhac})(\text{Hdmpz})]$  is depicted in Fig. 1. The bond parameters associated with the metal ion are listed in Table 2. The copper(II) centre is in a square-planar  $\text{N}_2\text{O}_2$  coordination environment constituted by the enolate-O, the imine-N and the deprotonated amide-O coordinating  $\text{bhac}^{2-}$  and the imine-N coordinating Hdmpz. The N2–C6 [1.304(3) Å] and C6–O2 [1.300(3) Å] distances are consistent with the deprotonated form of the amide functionality in  $\text{bhac}^{2-}$ .<sup>4,5,13,14</sup> The C2–C3 [1.363(4) Å] and C2–O1 [1.300(3) Å] distances indicate the enolate form of the  $-\text{HC}=\text{C}(\text{CH}_3)-\text{O}^-$  fragment of  $\text{bhac}^{2-}$ .<sup>16</sup> The chelate bite angles for the five- and six-membered rings formed by  $\text{bhac}^{2-}$  are  $81.66(8)$  and  $93.75(8)^\circ$ , respectively. The  $\text{Cu(II)}-\text{O}(\text{amide})$  distance [1.9168(18)

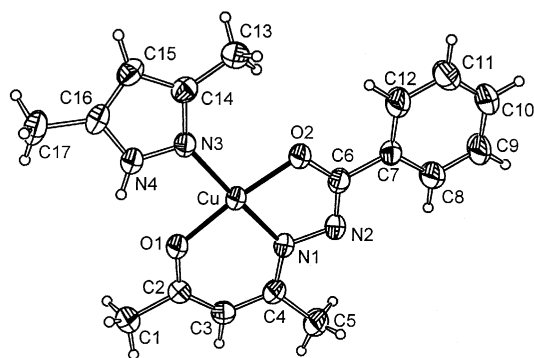


**Fig. 1** Molecular structure of [Cu(bhac)(Hdmpz)] and the atom labeling scheme. All non-hydrogen atoms are represented by their 50% probability thermal ellipsoids.

Å] is shorter than the distances [1.976(2)–2.063(2) Å] found in copper(II) complexes in which the O-coordinating amide functionality is protonated<sup>4,14c</sup> and comparable with the distances [1.914(4)–1.989(5) Å] observed for complexes in which the copper(II) is coordinated to deprotonated amide-O.<sup>14a,b</sup> The Cu(II)–N(imine) distance [1.915(2) Å] is unexceptional.<sup>14,16</sup> The Cu–O1 distance [1.9123(18) Å] is within the range reported for copper(II) to enolate-O bonds.<sup>16</sup> The Cu–N3 distance [1.998(2) Å] is similar to the values observed for copper(II) species containing a non-bridging neutral pyrazole moiety.<sup>17</sup> There is no displacement of the metal ion from the N<sub>2</sub>O<sub>2</sub> square-plane. The maximum and minimum deviations from the CuN<sub>2</sub>O<sub>2</sub> mean plane are 0.047(1) and 0.012(1) Å for O2 and Cu, respectively. The whole {Cu(bhac)} fragment is essentially planar, barring an insignificant twisting [by 3.03(11)°] of the phenyl ring plane (mean deviation 0.002 Å) with respect to the plane containing the rest of the atoms (Cu, O1, O2, N1, N2, C1–C6; mean deviation 0.033 Å). However, the Hdmpz plane (mean deviation 0.002 Å) has a different orientation with respect to the above mentioned plane. The dihedral angle between these two mean planes is 11.53(10)°.

### Self-assembly of [Cu(bhac)(Hdmpz)]

Very often in square-planar copper(II) complexes the metal ion is involved in weak interactions at the apical position with another atom of a neighbouring molecule, forming dimeric units or polymeric chains having equatorial-apical bridges.<sup>14a</sup> The metal ion is also displaced towards the apical atom from the square base in these complexes. In the present complex, other than the four coordinating atoms, the nearest atom to the metal ion is the metal-coordinated pyrazole-N of another molecule and the distance separating them is 3.275(2) Å. Considering this distance, the essentially planar CuN<sub>2</sub>O<sub>2</sub> fragment and the sp<sup>2</sup> character of the pyrazole-N already coordinated to another metal centre, any kind of weak interaction and hence dimerization or polymerization *via* equatorial-apical bridges can be ruled out. However, the [Cu(bhac)(Hdmpz)] molecules form a one-dimensional assembly through  $\pi$ - $\pi$  interactions. This one-dimensional arrangement in the crystal lattice is illustrated in Fig. 2. Each square-planar molecule is involved in two types of  $\pi$ - $\pi$  interactions with the two adjacent molecules.

**Table 2** Selected bond lengths (Å) and angles (°) for [Cu(bhac)(Hdmpz)]

Cu–O(1)	1.9123(18)	Cu–O(2)	1.9168(18)
Cu–N(1)	1.915(2)	Cu–N(3)	1.998(2)
O(1)–Cu–O(2)	174.20(7)	O(1)–Cu–N(1)	93.75(8)
O(1)–Cu–N(3)	88.18(8)	O(2)–Cu–N(1)	81.66(8)
O(2)–Cu–N(3)	96.51(8)	N(1)–Cu–N(3)	177.51(9)

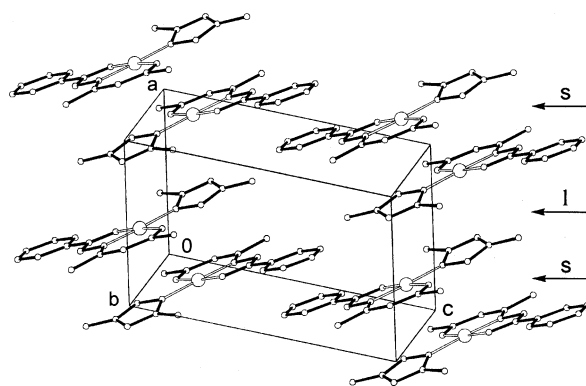


**Fig. 2** One-dimensional arrangement of  $\pi$ -stacked [Cu(bhac)(Hdmpz)] molecules in the crystal lattice. The arrows indicate short (s) and long (l) Cu···Cu distances.

This results in alternating short and long Cu···Cu distances in the chain-like arrangement of the metal ions. In the first type of interaction, the Hdmpz rings and the chelate rings of two molecules are involved in  $\pi$ - $\pi$  interactions in a reciprocal manner. The Cu···Cu distance observed is 3.5952(8) Å in this dimeric unit. The interplanar distances between the five- and the six-membered chelate rings and the Hdmpz ring are 3.232 and 3.406 Å, respectively. The corresponding centroid-to-centroid distances are 3.555 and 3.595 Å, respectively. The pyrazole ring is not exactly parallel with either of the five- or the six-membered chelate rings. The dihedral angles are 13.72° and 11.49°, respectively. In the second type of interaction, the Hdmpz rings of each of these dimeric units are overlapped with the Hdmpz rings of dimeric units on both sides and the interdimer Cu···Cu distance observed is 5.5960(12) Å (Fig. 2). The interplanar and the centroid-to-centroid distances between the pyrazole rings are 3.356 and 3.732 Å, respectively. The dihedral angle [0.0(1)°] between these pyrazole rings suggests that they are perfectly parallel.

There is no significant interchain interaction. Although the phenyl rings of the bhac<sup>2-</sup> moieties from two successive chains (Fig. 2) are parallel [dihedral angle 0.0(1)°] and the interplanar distance is 3.396 Å, a  $\pi$ - $\pi$  interaction can be ruled out considering the large (7.621 Å) centroid-to-centroid distance. The shortest C···C distance between two phenyl rings is 5.486(7) Å.

To examine whether or not any other crystalline form of the complex exists we have collected the powder X-ray diffraction pattern of the complex and compared it with the simulated diffraction pattern generated from the unit cell and the molecular structure determined by single crystal X-ray crystallography.<sup>18</sup> The experimental and simulated diffraction patterns are very similar with respect to the peak positions and the relative intensities (Fig. 3). This similarity indicates that the complex crystallizes only in one form having a chain-like arrangement of molecules with alternating short and long Cu···Cu distances in the crystal lattice.

### Magnetic susceptibility

Magnetic susceptibility measurements on a powdered sample of [Cu(bhac)(Hdmpz)] were performed in the temperature range of 10–300 K at a constant magnetic field of 5 kG. The effective magnetic moment ( $\mu_{\text{eff}}$ ) of the complex at 300 K is 1.94  $\mu_{\text{B}}$ . On cooling the moment gradually decreases. From 300 to 80 K the change in  $\mu_{\text{eff}}$  is small. At 80 K the value of  $\mu_{\text{eff}}$  is 1.87  $\mu_{\text{B}}$ . Below 80 K, the decrease in the value of  $\mu_{\text{eff}}$  is relatively sharp, falling to 1.35  $\mu_{\text{B}}$  at 10 K. The nature of the curve obtained by plotting the moments against temperature (Fig. 4) clearly indicates the antiferromagnetic behaviour of the complex. Considering the chain-like arrangement of the copper(II) centres with sequential long and short Cu···Cu distances in the

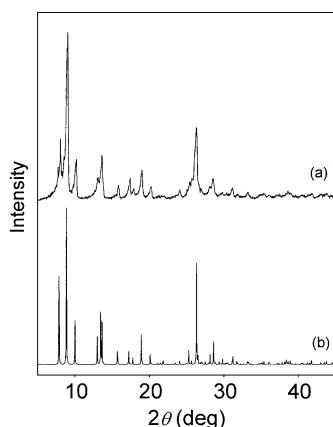


**Fig. 3** Powder X-ray diffraction pattern of [Cu(bhac)(Hdmpz)]: (a) experimental and (b) simulated.

solid state, we attempted to fit the data by using the alternating antiferromagnetic chain model.<sup>19</sup> The best least-squares<sup>20</sup> fit gave  $g = 2.207(3)$ ,  $J = -5.4(1) \text{ cm}^{-1}$ , and  $\alpha = 0.16(4)$  with a fixed TIP value of  $60 \times 10^{-6} \text{ emu mol}^{-1}$ , where  $J$  and  $J'$  are the antiferromagnetic coupling constants,  $\alpha = J'/J$  and TIP is the temperature independent paramagnetism. Since these values suggest that  $J'$  is very small, the data were also fitted using the Bleaney–Bowers expression.<sup>21</sup> The best least-squares fit was obtained with  $g = 2.217(1)$ ,  $J = -6.0(1) \text{ cm}^{-1}$ , and  $\text{TIP} = 60 \times 10^{-6} \text{ emu mol}^{-1}$ . This fit is noticeably better than that obtained by using the alternating antiferromagnetic chain model (Fig. 4).

### EPR spectra

The room temperature (298 K) X-band EPR spectral profile of the powdered complex is characteristic for a spin-coupled dicopper(II) species. A broad and strong asymmetric signal at  $g = 2.08$  and a weak absorption at  $g = 4.26$  are observed (Fig. 5, trace a). The former is assigned to the  $\Delta M_s = \pm 1$  transition and the latter to the  $\Delta M_s = \pm 2$  transition.<sup>22,23</sup> Lowering the temperature to 110 K sharpens the  $g = 2.08$  signal but decreases the intensity of the  $g = 4.26$  signal, suggesting an antiferromagnetically coupled system.

In solution, if the spin-coupled dicopper(II) species exists at room temperature a seven-line pattern at  $g \sim 2$  is expected.<sup>22b</sup> However, a  $\text{CHCl}_3\text{-C}_6\text{H}_5\text{CH}_3$  (1:1) solution of the complex

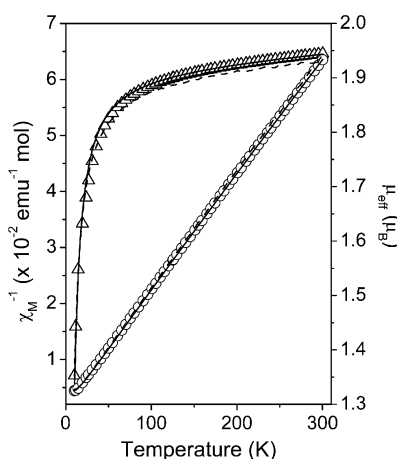


**Fig. 4** Inverse molar magnetic susceptibility (O) and effective magnetic moment ( $\Delta$ ) of [Cu(bhac)(Hdmpz)] as a function of temperature. The solid and the dashed lines represent the quality of the least-squares fits using the Bleaney–Bowers expression and the alternating antiferromagnetic chain model, respectively.

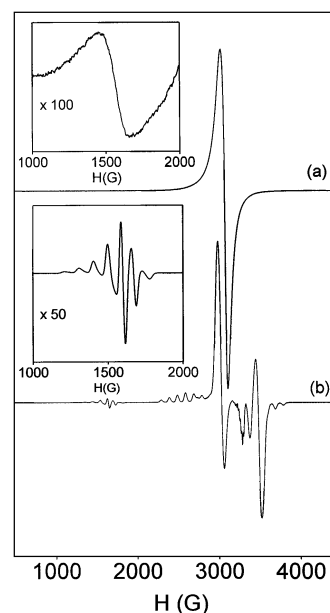


**Fig. 5** EPR spectra of [Cu(bhac)(Hdmpz)]: (a) in powder phase at 298 K, (b) in frozen (110 K) chloroform–toluene (1:1) solution ( $1.01 \times 10^{-1} \text{ M}$ ). Insets: Magnified  $\Delta M_s = \pm 2$  region for the powder phase (top) and that for the frozen solution (bottom).

at 298 K gives a typical isotropic spectrum with a four-line pattern ( $g = 2.09$ ,  $A = 88 \text{ G}$ ) for an uncoupled mononuclear copper(II) species.<sup>22a</sup> In dilute conditions the nitrogen superhyperfine lines are clearly visible on the high-field line.

The EPR spectra of frozen (110 K)  $\text{CHCl}_3\text{-C}_6\text{H}_5\text{CH}_3$  (1:1) solutions of the complex having different concentrations have been recorded. The spectrum of the complex at the highest concentration is depicted in Fig. 5, trace b. The spectral features are characteristic of two interacting copper(II) ions. The half-field transition is observed as a seven-line pattern with an average line spacing of 96 G at  $g = 4.39$ . The  $\Delta M_s = \pm 1$  transitions are observed in the range of 2200–3750 G. Observation of two pairs of transitions in this range due to zero-field splitting are consistent with an essentially axial symmetry. Seven copper hyperfine lines with an average line spacing of 99 G are readily apparent in the range of 2200–2850 G. Three absorptions with an average line separation of 96 G observed in the range of 3500–3800 G are assigned to the second seven-line pattern. The other four lines are presumably obscured by the preceding strong signal. These two seven-line patterns centred at 3458 and 2552 G are assigned to the parallel signals. The perpendicular components appear as two strong signals at 2984 and 3444 G. In between these two signals, two more signals are observed at  $\sim 3268$  and  $\sim 3375 \text{ G}$ . The signal at lower field is split by several lines. As the concentration decreases, the intensity of each of these two signals increases. On the other hand, there is a decrease in the intensities of the signals at 2984 and 3444 G, the seven-line patterns of the parallel components and the half-field signal. These decreasing signals are associated with the spin-coupled dicopper(II) species. Fig. 6 depicts this concentration dependent change of the signals in the  $\Delta M_s = \pm 1$  region. The major features in the spectrum of the complex at the lowest concentration (Fig. 6, trace d) are typical for an axial spectrum of a mononuclear square-planar copper(II) complex.<sup>22a</sup> The  $g_{\parallel}$  and  $A_{\parallel}$  values are 2.19 and 212 G, respectively. The  $g_{\perp}$  signal observed at 2.06 is split by several lines with an average line separation of 16 G. As the metal ion is coordinated to two different types of nitrogen atoms, nine nitrogen superhyperfine lines are expected. Eight lines are clearly visible in the  $g_{\perp}$  signal. Two weak absorptions are observed at  $\sim 2950$  and  $\sim 3480 \text{ G}$  (Fig. 6, trace d). Comparison of all the frozen solution spectra clearly suggests that these two



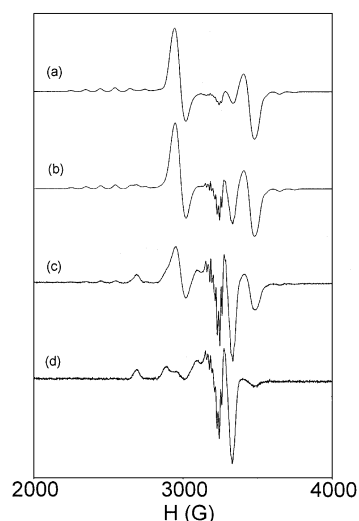


**Fig. 6**  $\Delta M_s = \pm 1$  region in the EPR spectra of [Cu(bhac)(Hdmpz)] in frozen (110 K) chloroform-toluene (1:1) solution: (a)  $1.01 \times 10^{-1}$  M, (b)  $1.01 \times 10^{-2}$  M, (c)  $1.01 \times 10^{-3}$  M, (d)  $1.01 \times 10^{-4}$  M.

weak absorptions are the perpendicular components of the  $\Delta M_s = \pm 1$  transitions from a small amount of the dicopper(II) species. Similarly, the signals at  $\sim 3268$  and  $\sim 3375$  G in the spectrum (Fig. 6, trace a) of the complex at the highest concentration indicate the presence of a small amount of uncoupled mononuclear copper(II) complex.

All the EPR spectra described above suggest that the spin-coupled dicopper(II) species exists not only in the solid state, but also in frozen solutions. The concentration dependent change of the spectral profiles clearly indicates the aggregation of [Cu(bhac)(Hdmpz)] molecules into a dimeric species at high concentrations. However, a small fraction of the molecules remains uncoupled. On the other hand, at low concentration, except for a small fraction most of the molecules remain uncoupled. The frozen solution EPR data can be used to calculate an approximate value for the Cu...Cu distance in the dicopper(II) species. In the  $\Delta M_s = \pm 1$  region of the EPR spectrum, the spacing between the two parallel components is  $2D_{\parallel}$ , where  $D_{\parallel}$  is the zero-field splitting parameter. According to our assignments of the signals in the frozen solution spectrum (Fig. 6, trace a), the separation between the parallel components is 906 G. The value of  $D_{\parallel}$  ( $453 \text{ G} = 0.041 \text{ cm}^{-1}$ ) is the sum of the zero-field splitting parameters due to dipole-dipole ( $D_{\text{dd}}$ ) and pseudo-dipolar ( $D_{\text{pd}}$ ) interactions. The magnitude of the pseudo-dipolar interaction depends on the extent of spin-exchange and magnetic anisotropy.<sup>21,22</sup> The relationship of  $D_{\text{pd}}$  with the spin-coupling constant  $J$ ,  $g_{\parallel}$ , and  $g_{\perp}$  is as follows:  $D_{\text{pd}} = 2J\{[(g_{\parallel} - 2)^2/4] - (g_{\perp} - 2)^2\}/8$ . From this relation the value of  $D_{\text{pd}}$  has been evaluated as  $-9.8 \times 10^{-3} \text{ cm}^{-1}$  using the values of  $J$  ( $-6.0 \text{ cm}^{-1}$ ),  $g_{\parallel}$  (2.19) and  $g_{\perp}$  (2.05). Thus,  $D_{\text{dd}}$  is obtained as  $0.051 \text{ cm}^{-1}$  by subtraction of  $D_{\text{pd}}$  from  $D_{\parallel}$ . Using these values of  $D_{\text{dd}}$  and  $g_{\parallel}$  in the equation<sup>22,24</sup>  $R^3 = 0.65 g_{\parallel}^2 / D_{\text{dd}}$  the Cu...Cu distance ( $R$ ) in the dicopper(II) species in frozen solution is evaluated as 3.94 Å.

## Conclusion

The synthesis, structure and properties of a mixed-ligand square-planar copper(II) complex, [Cu(bhac)(Hdmpz)], have been described. In the solid state, each complex molecule is involved in reciprocal  $\pi$ -overlapping of the chelate rings and Hdmpz rings with one neighbour (short Cu...Cu distance) and in another  $\pi$ -overlapping of the Hdmpz rings only with the other neighbour (long Cu...Cu distance) (Fig. 2) forming a chain-like arrangement of the metal ions. Solid state variable

temperature magnetic susceptibility measurements and the EPR spectra of the complex in powder phase as well as in frozen solution indicate a weakly coupled dicopper(II) species. The X-ray structure shows that there is no deviation of the metal centre from the square-plane formed by the four coordinating atoms. In addition, each molecule in the one-dimensional arrangement is laterally displaced with respect to its neighbouring molecules on both sides. Consequently, a direct Cu...Cu interaction can be ruled out as the origin of the observed weak antiferromagnetic interaction. Thus, the readily apparent pathway, at least in the solid state, for the observed antiferromagnetic spin-coupling is a superexchange *via* the electrons involved in the  $\pi$ - $\pi$  interaction. The antiferromagnetic interaction between the more closely spaced metal ions is expected to be much stronger as the chelate rings containing these metal ions are involved in  $\pi$ - $\pi$  interactions with the coordinated Hdmpz rings. Most likely this dimeric unit is reflected in the magnetic susceptibility and EPR data. Thus, the one-dimensional arrangement in the solid state can be viewed as the  $\pi$ -stacked assembly of this spin-coupled dimeric unit that itself is formed by  $\pi$ - $\pi$  interactions. Within this chain of dimers, there is essentially no interdimer spin exchange.

Unlike in the solid state, existence of a typical dimeric Cu(II) species formed by mutual involvement of two molecules in equatorial-apical bridging through metal coordinated N or O atoms cannot be ruled out in frozen solution. However, the value of Cu...Cu distance (3.94 Å) calculated from the frozen solution EPR data is very close to the short Cu...Cu distance [3.5958(8) Å] observed in the one-dimensional arrangement of the molecules in the solid state. Thus, as observed in the solid state, formation of dimeric aggregates of [Cu(bhac)(Hdmpz)] molecules by  $\pi$ -overlapping is a distinct possibility in frozen solution. Similar  $\pi$ -stacking of organic ion radicals in solution phase was reported earlier.<sup>25</sup>

Magnetic exchange interactions *via* non-covalent weak intermolecular interactions such as van der Waals, hydrogen-bonding and  $\pi$ -stacking in supramolecular species formed by the same non-covalent intermolecular interactions is of considerable current interest.<sup>26,27</sup> Very few complexes are known in which magnetic exchange occurs solely through intermolecular  $\pi$ - $\pi$  interactions involving the terminal aromatic ligands.<sup>27</sup> To the best of our knowledge the present complex provides a unique example of metal ion spin-coupling in a square-planar copper(II) complex where  $\pi$ -overlapping of the chelate rings and unidentate heterocycles of two molecules helps to form a dimeric unit and provides the superexchange pathway. The only other example reported for copper(II) spin-exchange in a similar way is a dimeric aggregate of the non-planar anionic complex [Cu(mnt)<sub>2</sub>]<sup>2-</sup> where mnt<sup>2-</sup> is maleonitriledithiolate.<sup>28</sup>

## Acknowledgements

Financial support for this work was provided by the Department of Science and Technology (DST), New Delhi (Grant No. SP/S1/F23/99). The X-ray structure determination was performed at the DST funded National Single Crystal Diffractometer Facility, School of Chemistry, University of Hyderabad. We thank the University Grants Commission, New Delhi, for the facilities provided under the UPE program. We are grateful to Prof. A. R. Chakravarty for providing the cryomagnetic data. We thank Prof. M. V. Rajasekharan for several discussions and suggestions. Mr. S. Das and Mr. Sataynarayan Pal thank the Council of Scientific and Industrial Research, New Delhi for research fellowships.

## References

- 1 Proceedings of the Inorganic Crystal Engineering (Dalton Discussion No. 3) in: *J. Chem. Soc., Dalton Trans.*, 2000, 3705–3998..

- 2 (a) T. J. Marks, *Angew. Chem., Int. Ed. Engl.*, 1990, **29**, 857; (b) T. Mallah, S. Thiébaud, M. Verdaguer and P. Veillet, *Science*, 1993, **262**, 1554; (c) O. Kahn and C. J. Martinez, *Science*, 1998, **279**, 44; (d) B. Schoentjes and J.-M. Lehn, *Helv. Chim. Acta*, 1995, **78**, 1; (e) O. R. Evans and W. Lin, *Acc. Chem. Res.*, 2002, **35**, 511.
- 3 (a) P. N. W. Baxter, J.-M. Lehn, B. O. Kneisel and D. Fenske, *Angew. Chem., Int. Ed. Engl.*, 1997, **36**, 1978; (b) D. Braga, F. Grepioni and G. R. Desiraju, *Chem. Rev.*, 1998, **98**, 1375; (c) R. J. Puddephatt, *Chem. Commun.*, 1998, 1055; (d) C. Janiak, *J. Chem. Soc., Dalton Trans.*, 2000, 3885.
- 4 N. R. Sangeetha, S. N. Pal, C. E. Anson, A. K. Powell and S. Pal, *Inorg. Chem. Commun.*, 2000, **3**, 415.
- 5 N. R. Sangeetha, C. K. Pal, P. Ghosh and S. Pal, *J. Chem. Soc., Dalton Trans.*, 1996, 3293.
- 6 W. E. Hatfield, in *Theory and Applications of Molecular Paramagnetism*, eds. E. A. Boudreaux and L. N. Mulay, Wiley, New York, 1976, p. 491.
- 7 A. C. T. North, D. C. Philips and F. S. Mathews, *Acta Crystallogr., Sect. A*, 1968, **24**, 351.
- 8 L. J. Farrugia, *J. Appl. Crystallogr.*, 1999, **32**, 837.
- 9 G. M. Sheldrick, *SHELX-97 Structure Determination Software*, University of Göttingen, Göttingen, Germany, 1997.
- 10 P. McArdle, *J. Appl. Crystallogr.*, 1995, **28**, 65.
- 11 A. L. Spek, *Platon98 Molecular Graphics Software*, University of Glasgow, UK, 1998.
- 12 K. Nakamoto, *Infrared and Raman Spectra of Inorganic and Coordination Compounds*, Wiley, New York, 1986, pp. 241–244.
- 13 S. N. Pal and S. Pal, *J. Chem. Soc., Dalton Trans.*, 2002, 2102.
- 14 (a) N. R. Sangeetha and S. Pal, *Polyhedron*, 2000, **19**, 1593; (b) N. R. Sangeetha, K. Baradi, R. Gupta, C. K. Pal, V. Manivannan and S. Pal, *Polyhedron*, 1999, **18**, 1425; (c) N. R. Sangeetha and S. Pal, *J. Chem. Crystallogr.*, 1999, **29**, 287.
- 15 S. N. Pal and S. Pal, *Inorg. Chem.*, 2001, **40**, 4807.
- 16 (a) R. Clark, D. Hall and T. N. Waters, *J. Chem. Soc. A*, 1969, 823; (b) A. Mederos, A. Medina, E. Medina, F. G. Manrique, P. Nunez and M. L. Rodriguez, *J. Coord. Chem.*, 1987, **15**, 393; (c) J. T. Pulkkinen, R. Laatikainen, M. J. Ahlgren, M. Peräkylä and J. J. Vepsäläinen, *J. Chem. Soc., Perkin Trans. 2*, 2000, 777; (d) Y.-P. Cai, C.-Y. Su, A.-W. Xu, B.-S. Kang, Y.-X. Tong, H.-Q. Liu and S. Jie, *Polyhedron*, 2001, **20**, 657.
- 17 M. K. Elhert, S. J. Rettig, A. Storr, R. C. Thompson and J. Trotter, *Can. J. Chem.*, 1992, **70**, 2161.
- 18 W. Kraus and G. Nolze, *PowderCell 2.3*, Federal Institute for Materials Research and Testing, Berlin, Germany, 1999.
- 19 (a) W. E. Hatfield, *J. Appl. Phys.*, 1981, **52**, 1985; (b) J. W. Hall, W. E. Marsh, R. R. Weller and W. E. Hatfield, *Inorg. Chem.*, 1981, **20**, 1033.
- 20 G. V. R. Chandramouli, C. Balagopalakrishna, M. V. Rajasekharan and P. T. Manoharan, *Comput. Chem.*, 1996, **20**, 353.
- 21 B. Bleay and K. D. Bowers, *Proc. R. Soc. London, Ser. A*, 1952, **214**, 451.
- 22 (a) E. F. Hasty, T. J. Colburn and D. N. Hendrickson, *Inorg. Chem.*, 1973, **12**, 2414; (b) E. F. Hasty, L. J. Wilson and D. N. Hendrickson, *Inorg. Chem.*, 1978, **17**, 1834.
- 23 (a) A. M. Greenaway, C. J. O'Connor, J. W. Overman and E. Sinn, *Inorg. Chem.*, 1981, **20**, 1508; (b) J.-P. Costes, F. Dahan and J.-P. Laurent, *Inorg. Chem.*, 1985, **24**, 1018.
- 24 K. W. H. Stevens, *Proc. R. Soc. London, Ser. A*, 1952, **214**, 237.
- 25 (a) J.-F. Penneau, B. J. Stallman, P. H. Kasai and L. L. Miller, *Chem. Mater.*, 1991, **3**, 791; (b) C. J. Zhong, W. S. V. Kwan and L. L. Miller, *Chem. Mater.*, 1992, **4**, 1423; (c) M. E. Benz, I. Tabakovic and L. L. Miller, *Chem. Mater.*, 1994, **6**, 351; (d) L. L. Miller, T. Hashimoto, I. Tabakovic, D. R. Swanson and D. A. Tomalia, *Chem. Mater.*, 1995, **7**, 9.
- 26 (a) O. Kahn, Y. Pei and Y. Journaux, in *Inorganic Materials*, eds. D. W. Bruce and D. O'Hare, Wiley, Chichester, 1992, p. 59; (b) C. Kollmar and O. Kahn, *Acc. Chem. Res.*, 1993, **26**, 259; (c) P. A. Goodson, J. Glerup, D. J. Hodgson, K. Michelsen and U. Rychlewski, *Inorg. Chem.*, 1994, **33**, 359; (d) M. C. Morón, F. Palacio, J. Pons, J. Casabó, X. Solans, K. E. Merabet, D. Huang, X. Shi, B. K. Teo and R. L. Carlin, *Inorg. Chem.*, 1994, **33**, 746; (e) J. S. Miller and A. J. Epstein, *Angew. Chem., Int. Ed. Engl.*, 1994, **33**, 385.
- 27 (a) M. Wesolek, D. Meyer, J. A. Osborn, A. De Cian, J. Fischer, A. Derory, P. Legoll and M. Drillon, *Angew. Chem., Int. Ed. Engl.*, 1994, **33**, 1592; (b) A. J. Amoroso, J. C. Jeffery, P. L. Jones, J. A. McCleverty, P. Thornton and M. D. Ward, *Angew. Chem., Int. Ed. Engl.*, 1995, **34**, 1443; (c) M. C. Muñoz, M. Julve, F. Lloret, J. Faus and M. Andruh, *J. Chem. Soc., Dalton Trans.*, 1998, 3125; (d) S. Tanase, M. Ferbinteanu, M. Andruh, C. Mathonière, I. Strenger and G. Rombaut, *Polyhedron*, 2000, **19**, 1967.
- 28 D. Snaathorst, H. M. Doesburg, J. A. A. J. Perenboom and C. P. Keijzers, *Inorg. Chem.*, 1981, **20**, 2526.